Asian Journal of Chemistry; Vol. 38, No. 2 (2026), 417-424
ASIAN JOURNAL OF CHEMISTRY
https://doi.org/10.14233/ajchem.2026.35047

Synthesis, Antimicrobial and DFT Studies of 1,3,4-Oxadiazole Linked Quinoline Carbaldehyde Derivatives

JANARDHANA NAYAK[1,*] and JYOTHI KUDVA[2]

[1]Department of Chemistry, NMAM Institute of Technology, Nitte (Deemed to be University), Nitte-574110, India
[2]Department of Chemistry, St. Joseph Engineering College (Affiliated to Visvesvaraya Technological University, Belagavi), Mangaluru-575028, India

*Corresponding author: E-mail: jnayak@nitte.edu.in

Received: 10 October 2025 *Accepted*: 8 January 2026 *Published online*: 31 January 2026 AJC-22259

A novel series of oxadiazole-linked quinoline derivatives was synthesized and evaluated for antimicrobial activity and electronic properties. The synthetic pathway involved the preparation of 4-substituted benzohydrazides, subsequent cyclization to yield 5-(4-substituted phenyl)-1,3,4-oxadiazole-2-thiols, and their coupling with 6/8-substituted-2-chloroquinoline-3-carbaldehydes to obtain the target compounds *viz.* 2-((5-(4-substituted phenyl)-1,3,4-oxadiazol-2-yl)thio)-6/8-substituted quinoline-3-carbaldehydes (**7a-l**) in moderate to good yields. Antibacterial activity was assessed against *Staphylococcus aureus*, *Bacillus subtilis*, *Escherichia coli* and *Pseudomonas aeruginosa*, while antifungal activity was evaluated against *Candida albicans* using minimum inhibitory concentration (MIC) methods. Most compounds exhibited promising antimicrobial activity. Notably, compounds **7g** and **7k**, bearing *p*-nitro phenyl substitution on the oxadiazole ring and chloro substitution on the quinoline nucleus, showed superior antibacterial and antifungal activities comparable to standard drugs.

Keywords: Oxadiazole–quinoline hybrids, Antimicrobial activity, Density functional theory, HOMO-LUMO analysis.

INTRODUCTION

Nitrogen-containing heterocycles constitute a foundation of medicinal chemistry owing to their privileged scaffold status, synthetic tractability and broad pharmacological profiles [1-3]. Among these, quinoline frameworks are especially remarkable as they reinforce multiple clinically relevant agents and investigational leads across infectious, inflammatory, oncologic and cardiovascular indications [4,5]. The quinoline ring exhibits diverse biological activities, including anti-tuberculosis [6], antimalarial [7], anti-inflammatory [8], anticancer [9], antibiotic [10] and antihypertensive effects [11]. Mechanistically, quinoline derivatives have also been implicated in tyrosine kinase PDGF-RTK inhibition [12] and anti-HIV activity [13,14], underscoring the scaffold's capacity to engage targets spanning enzymatic, receptor-mediated and nucleic acid-associated processes. This extensiveness of activity, coupled with the tunable electronics and sterics of the fused benzopyridine core, continues to motivate the design of quinoline-based hybrid molecules aimed at enhanced potency, selectivity and pharmacokinetic properties.

In parallel, the 1,3,4-oxadiazole motif has also garnered sustained attention as a bioisostere and linker in drug design, valued for its metabolic stability, hydrogen-bonding capacity and electron-withdrawing character that can modulate physicochemical and ADMET attributes [15,16]. Derivatives of 1,3,4-oxadiazole also display antimicrobial [17,18], anti-HIV [19], antitubercular [20], antimalarial [21], anti-inflammatory [22,23], anticonvulsant [24] and antitumor activities [25]. Strategically, incorporating oxadiazoles into pharmacophore architectures can (i) refine dipole moments and lipophilicity for membrane permeability, (ii) adjust π-electron distribution to optimize target binding and (iii) introduce the conformational constraints that favour productive bioactive poses [26,27]. Consequently, the oxadiazole-bridged hybrids have emerged as a rational design avenue for elevating antimicrobial efficacy while balancing drug-like properties [28,29].

Recent efforts illustrate the combinatorial value of integrating these two privileged motifs. Quinoline derivatives bearing 1,3,4-oxadiazole-bridged pyrazole or isoxazole moieties have been designed, synthesized and validated for antimicrobial and anti-inflammatory activities, with molecular docking supp-

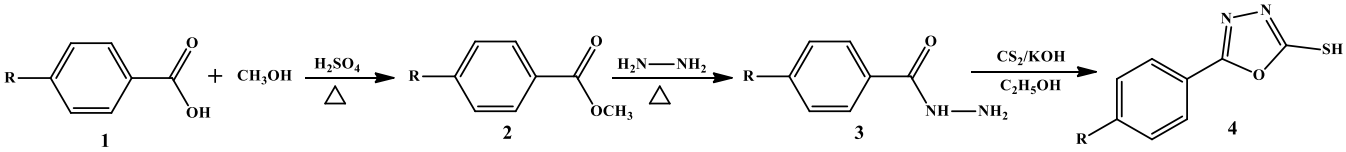

Scheme-I: Synthesis of 5-(4-substituted phenyl)-1,3,4-oxadiazole-2-thiols (**4**)

orting plausible binding hypotheses and target engagement [30]. Likewise, novel quinoline-substituted 1,3,4-oxadiazole derivatives have been reported with robust antimicrobial and anti-inflammatory profiles [31]. Together, these studies signal that hybridization of quinoline with oxadiazole can be a fruitful strategy for multi-target modulation, enabling fine control over electronic features and heteroatom placement to strengthen interactions with microbial enzymes, receptors and cell wall components. Beyond activity, the oxadiazole linker can also serve to improve chemical stability and reduce off-target liabilities, key considerations for translational potential.

Based on this foundation, our earlier reports on the one-pot synthesis of 2-(4-substituted phenyl)-6/8-substituted [1,3,4]oxadiazolo[2′,3′:2,3][1,3]thiazino[6,5-*b*]quinolin-11-(3a*H*)-ones *via* coupling of 5-(4-substituted phenyl)-1,3,4-oxadiazole-2-thiols with 6/8-substituted-2-chloroquinoline-3-carboxylic acids in the presence of sodium acetate and ethanol [32]. The results demonstrated that oxadiazole-quinoline fusion is synthetically accessible under relatively mild conditions and that electron-withdrawing substituents can beneficially influence the biological activity. In light of the above, and as a continuation of our previous work [32], we sought to systematically synthesize oxadiazole-linked quinolines with tailored substitution patterns designed to enhance antimicrobial potency.

EXPERIMENTAL

The melting points of the newly synthesised compounds were determined in open capillaries using Bio-Techniques India BTI-39 melting point instrument and are uncorrected. The IR spectra were recorded on an Agilent Technologies FT-IR spectrophotometer. The ^{1}H NMR and ^{13}C NMR spectra were recorded on a Bruker 400 MHz and 100 MHz, respectively NMR spectrometer using DMSO as solvent and TMS as internal standard. Mass spectra of some selected compounds were recorded on a WATERS Micromass ZQ HRMS Mass spectrometer. The purity of all new compounds was checked by thin layer chromatography (TLC) using glass plate coated with silica gel-G and spots were detected by iodine vapours.

General procedure for the synthesis of 4-substituted benzohydrazides (3): A mixture of 4-substituted benzoic acid (**1**) (0.246 mol), methanol (115 mL) and conc. H_2SO_4 (2.7 mL) was refluxed for 8-10 h. After this, the excess methanol was distilled out, then the resulting mixture was poured into ice-cold water and finally extracted with ether. Excess ether was eliminated by evaporation, yielding a crude solid of methyl-4-substituted benzoate, which was subsequently purified through distillation. In next step, a mixture of methyl-4-substituted benzoates (**2**) (0.1 mol) and hydrazine hydrate (5 mL, 0.1 mol) was heated in 40 mL of ethanol on a water bath for 8 h. Upon cooling, a solid mass of 4-substituted benzohydrazides (**3**) was obtained, collected through filtration, washed with water and then recrystallised using 30% ethanol. (yield 65%).

Synthesis of 5-(4-substituted phenyl)-1,3,4-oxadiazole-2-thiols (4): In a 250 mL flask, 4-substituted benzohydrazides (**3**) (7 g, 0.038 mol) were dissolved in 40 mL of absolute ethanol. Next, 2 mL of carbon disulfide (0.034 mol) was added to the solution, followed by a solution of KOH (1.2 g, 0.019 mol) in 20 mL of water. The reaction mixture was stirred thoroughly and refluxed for 5-6 h, during which H_2S gas was evolved. Once the reaction was complete, excess ethanol was removed under reduced pressure. The resulting mixture was diluted with 200 mL of distilled water and acidified to pH 2-3 using 4 N HCl. Finally, the mixture was filtered, washed with diethyl ether and recrystallised from ethanol (**Scheme-I**) (yield: 65%).

Synthesis of 6/8-substituted-2-chloroquinoline-3-carbaldehydes (6): Dimethylformamide (9.9 mL, 0.125 mol) was cooled to 0 ºC in a flask fitted with a drying tube, after which phosphoryl chloride (32.2 mL, 0.35 mol) was added dropwise with stirring. The substituted acetanilide (**5**) (6.55 g, 0.05 mol) was then introduced into the mixture, which was heated under reflux for 16 h. After the reaction was complete, the product was added to ice water and stirred for 30 min at 0-10 ºC, resulting in the separation of 6/8-substituted-2-chloroquinoline-3-carbaldehydes (**6**). It was filtered, washed with water and recrystallised from ethyl acetate (**Scheme-II**) (yield: 68%).

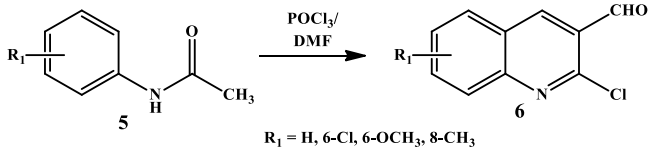

Scheme-II: Synthesis of 6/8-substituted-2-chloroquinoline-3-carbaldehydes (**6**)

Synthesis of 2-((5-(4-substituted phenyl)-1,3,4-oxadiazol-2-yl)thio)-6/8-substituted quinoline-3-carbaldehydes (7): A mixture 5-(4-substituted phenyl)-1,3,4-oxadiazole-2-thiols (**4**) (0.01 mol) and 6/8-substituted-2-chloro quinoline-3-carbaldehydes (**6**) (0.01 mol) were dissolved in ethanol (20 mL). Pyridine (1 mL) was added as a catalyst to the above mixture and the contents were refluxed on water bath for 4 to 5 h. After completion of the reaction, the excess solvent was removed by distillation and the contents were cooled to room temperature. The solid product separated was collected by filtration, dried and recrystallised from a mixture of ethanol and dimethylformamide (**Scheme-III**).

2-((5-Phenyl-1,3,4-oxadiazol-2-yl)thio)quinoline-3-carbaldehyde (7a): Yield: 76%, m.p.: 213-215 ºC; FT-IR (KBr, ν_{max}, cm^{-1}): 3169.89-2758.58 (aromatic C–H *str.*), 1689.6 (aldehyde C=O *str.*), 1562.10-1534.32 (oxadiazole and quin-

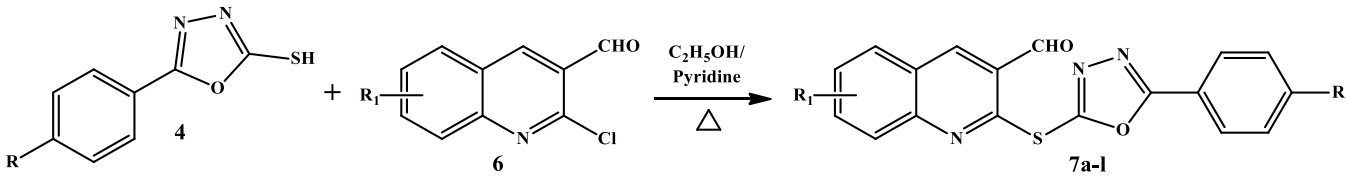

Scheme-III: 2-((5-(4-Substituted phenyl)-1,3,4-oxadiazol-2-yl)thio)-6/8- substituted quinoline-3-carbaldehyde (**7a-l**)

oline C=N *str*.), 1243.10 (oxadiazole C–O–C *str*.); ^{1}H NMR (DMSO, 400 MHz, δ ppm): 10.232 (s, 1H, –CHO), 9.142 (s, 1H, quinoline H-4), 7.62-8.36 (m, 9H, quinoline H-5, H-6, H-7, H-8 and phenyl protons); ^{13}C NMR (DMSO, 100 MHz, δ ppm): 192.995 (–CHO carbon atom), 123.320, 125.34, 126.273, 127.114, 127.019, 129.088, 130.130, 132.158, 133.160, 134.561, 135.453, 147.362, 147.399, 152.985, 159.928, 167.626, 168.220 (phenyl, quinoline and oxadiazole carbon atoms); HRMS *m/z*: 334.3638 (M^++1) (m.f.: $C_{18}H_{11}N_3O_2S$).

8-Methyl-2-((5-phenyl-1,3,4-oxadiazol-2-yl)thio)quinoline-3-carbaldehyde (7b): Yield: 74%, m.p.: 212-214 ºC; FT-IR (KBr, ν_{max}, cm^{-1}): 3037.8-2762.0 (aromatic C–H *str*.), 1677.3 (aldehyde C=O *str*.), 1677.3-1569.2 (oxadiazole and quinoline C=N *str*.), 1166.7 (oxadiazole C–S *str*.), 1080.9 (quinoline C–S *str*.), 1487.23 (quinoline C–CH_3 *def*.); ^{1}H NMR (DMSO, 400 MHz, δ ppm): 10.241 (s, 1H, –CHO), 9.123 (s, 1H, quinoline H-4), 8.015-8.048 (m, 2H, quinoline H-5 and H-7), 7.563-7.704 (m, 6H, quinoline H-8 and phenyl protons), 2.612 (s, 3H, quinoline CH_3); ^{13}C NMR (DMSO, 100 MHz, δ ppm): 192.994 (-CHO carbon atom), 16.614 (-CH_3 carbon atom), 123.319, 125.484, 126.273, 127.114, 128.019, 129.088, 130.130, 132.058, 133.060, 134.461, 135.353, 147.352, 147.389, 152.995, 159.828, 167.526, 168.120 (phenyl, quinoline and oxadiazole carbon atoms); HRMS, *m/z*: 348.5474 (M^++1) (m.f.: $C_{19}H_{13}N_3O_2S$).

6-Chloro-2-((5-phenyl-1,3,4-oxadiazol-2-yl)thio)quinoline-3-carbaldehyde (7c): Yield: 68%, m.p.: 254-256 ºC; FT-IR (KBr, ν_{max}, cm^{-1}): 3078.78-2879.5 (aromatic C–H *str*.), 1686.57 (aldehyde C=O *str*.), 1582.3-1562.10 (oxadiazole and quinoline C=N *str*.), 1264.10 (oxadiazole C–O–C *str*.), 778.98 (quinoline C–Cl *str*.); ^{1}H NMR (DMSO, 400 MHz, δ ppm): 10.232 (s, 1H, –CHO), 9.243 (s, 1H, quinoline H-4), 7.64-8.45 (m, 8H, quinoline H-5, H-6, H-7 and phenyl protons); ^{13}C NMR (DMSO, 100 MHz, δ ppm): 192.985 (–CHO carbon atom), 123.310, 125.340, 126.272, 127.124, 127.029, 129.087, 130.131, 132.168, 133.161, 134.562, 135.452, 147.361, 147.398, 152.986, 159.929, 167.625, 168.221 (phenyl, quinoline and oxadiazole carbon atoms); HRMS, *m/z*: 368.7069 (M^++1) (m.f.: $C_{18}H_{10}ClN_3O_2S$).

6-Methoxy-2-((5-phenyl-1,3,4-oxadiazol-2-yl)thio)-quinoline-3-carbaldehyde (7d): Yield: 69%, m.p.: 234-236 ºC; FT-IR (KBr, ν_{max}, cm^{-1}): 3059.78-2849.58 (aromatic C–H *str*.), 1698.7 (aldehyde C=O *str*.), 1576.32-1542.10 (oxadiazole and quinoline C=N *str*.), 1254.10 (oxadiazole C–O–C *str*.), 1365.56 (quinoline C-OCH_3 *str*.); ^{1}H NMR (DMSO, 400 MHz, δ ppm): 10. 232 (s, 1H, –CHO), 9.353 (s, 1H, quinoline H-4), 7.64-8.64 (m, 8H, quinoline H-5, H-6, H-7 and phenyl protons), 3.96 (s, 3H, OCH_3); ^{13}C NMR (DMSO, 100 MHz, δ ppm): 55.62 (–OCH_3 carbon atoms), 192.985 (–CHO carbon atom), 123.310, 125.340, 126.272, 127.124, 127.029, 129.087, 130.131, 132.168, 133.161, 134.562, 135.452, 147.361, 147.398, 152.986, 159.939, 167.635, 168.222 (phenyl, quinoline and oxadiazole carbon atoms). HRMS, *m/z*: 363.3765 (M^+) (m.f.: $C_{19}H_{13}N_3O_3S$).

2-((5-(4-Chlorophenyl)-1,3,4-oxadiazol-2-yl)thio)quinoline-3-carbaldehyde (7e): Yield: 72%, m.p.: 233-235 ºC; FT-IR (KBr, ν_{max}, cm^{-1}): 3059.78-2918.58 (aromatic C–H *str*.), 1694.5 (aldehyde C=O *str*.), 1576.32-1554.10 (oxadiazole and quinoline C=N *str*.), 1257.10 (oxadiazole C–O–C *str*.), 735.56 (phenyl C–Cl *str*.); ^{1}H NMR (DMSO, 400 MHz, δ ppm): 10.232 (s, 1H, –CHO), 9.142 (s, 1H, quinoline H-4), 7.58-8.28 (m, 8H, quinoline H-5, H-6, H-7, H-8 and phenyl protons); ^{13}C NMR (DMSO, 100 MHz, δ ppm): 192.985 (–CHO carbon atom), 123.420, 125.341, 126.373, 127.214, 127.119, 129.188, 130.120, 132.168, 133.161, 134.571, 135.463, 147.361, 147.398, 152.986, 159.929, 167.627, 168.221 (phenyl, quinoline and oxadiazole carbon atoms); HRMS, *m/z*: 368.4755 (M^++1) (m.f.: $C_{18}H_{10}ClN_3O_2S$).

2-((5-(4-Chlorophenyl)-1,3,4-oxadiazol-2-yl)thio)-8-methylquinoline-3-carbaldehyde (7f): Yield: 70%, m.p.: 286-288 ºC FT-IR (KBr, ν_{max}, cm^{-1}): 3048.58-2923.48 (aromatic C–H *str*.), 1688.7 (aldehyde C=O *str*.), 1581.21-1567.10 (oxadiazole and quinoline C=N *str*.), 1262.10 (oxadiazole C–O–C *str*.), 1487.23 (quinoline C–CH_3 *str*.), 735.56 (phenyl C–Cl *str*.); ^{1}H NMR (DMSO, 400 MHz, δ ppm): 2.621 (s, 3H, CH_3), 10.242 (s, 1H, –CHO), 9.132 (s, 1H, quinoline H-4), 7.55-8.08 (m, 7H, quinoline H-5, H-7, H-8 and phenyl protons); ^{13}C NMR (DMSO, 100 MHz, δ ppm): 16.615 (–CH_3 carbon atom), 192.995 (–CHO carbon atom), 123.319, 125.484, 126.273, 127.114, 128.019, 129.088, 130.130, 132.058, 133.060, 134.461, 135.353, 147.352, 147.389, 152.995, 159.828, 167.526, 168.120 (phenyl, quinoline and oxadiazole carbon atoms); HRMS, *m/z*: 382.7354 (M^++1) (m.f.: $C_{19}H_{12}ClN_3O_2S$).

6-Chloro-2-((5-(4-chlorophenyl)-1,3,4-oxadiazol-2-yl)-thio)quinoline-3-carbaldehyde (7g): Yield: 68%, m.p.: 293-295 ºC; FT-IR (KBr, ν_{max}, cm^{-1}): 3057.78-2956.48 (aromatic C–H *str*.), 1692.8 (aldehyde C=O *str*.), 1587.20-1571.20 (oxadiazole and quinoline C=N *str*.), 1263.10 (oxadiazole C–O–C *str*.), 755.5-735.56 (phenyl C–Cl and quinoline C–Cl *str*.); ^{1}H NMR (DMSO, 400 MHz, δ ppm): 10.1532 (s, 1H, –CHO), 9.232 (s, 1H, quinoline H-4), 7.65-8.64 (m, 7H, quinoline H-5, H-7, H-8 and phenyl protons); ^{13}C NMR (DMSO, 100 MHz, δ ppm): 192.985 (–CHO carbon atom), 123.320, 125.330, 126.282, 127.125, 127.030, 129.092, 130.132, 132.169, 133.162, 134.561, 135.462, 147.362, 147.399, 152.987, 159.930, 167.626, 168.223 (phenyl, quinoline and oxadiazole carbon atoms); HRMS, *m/z*: 404.2889 (M^++2) (m.f.: $C_{18}H_9Cl_2N_3O_2S$).

2-((5-(4-Chlorophenyl)-1,3,4-oxadiazol-2-yl)thio)-6-methoxyquinoline-3-carbaldehyde (7h): Yield: 67%, m.p.:

294-296 ºC; FT-IR (KBr, ν_{max}, cm^{-1}): 3062.75-2945.49 (aromatic C–H *str.*), 1694.7 (aldehyde C=O *str.*), 1587.20-1571.20 (oxadiazole and quinoline C=N *str.*), 1365.56 (quinoline C-OCH_3 *str.*). 1264.10 (oxadiazole C–O–C *str.*), 735.56 (phenyl C–Cl); ^{1}H NMR (DMSO, 400 MHz, δ ppm): 10.132 (s, 1H, –CHO), 8.96 (s, 1H, quinoline H-4), 7.65-7.90 (m, 7H, quinoline H-5, H-6, H-7 and phenyl protons), 3.97 (s, 1H, –OCH_3); ^{13}C NMR (DMSO, 100 MHz, δ ppm): 55.62 (–OCH_3 carbon atoms), 192.995 (–CHO carbon atom), 123.311, 125.330, 126.281, 127.132, 127.030, 129.097, 130.132, 132.169, 133.162, 134.562, 135.452, 147.362, 147.389, 152.986, 159.939, 167.635, 168.221 (phenyl, quinoline and oxadiazole carbon atoms); HRMS, *m/z*: 398.8449 (M^++1) (m.f.: $C_{19}H_{12}ClN_3O_3S$).

2-((5-(4-Nitrophenyl)-1,3,4-oxadiazol-2-yl)thio)quinoline-3-carbaldehyde (7i): Yield: 70%, m.p.: 228-230 ºC; FT-IR (KBr, ν_{max}, cm^{-1}): 3068.75-2953.49 (aromatic C–H *str.*), 1692.8 (aldehyde C=O *str.*), 1588.20-1572.20 (oxadiazole and quinoline C=N *str.*), 1530.56 (phenyl C-NO_2 *str.*). 1263.20; (oxadiazole C–O–C *str.*); ^{1}H NMR (DMSO, 400 MHz, δ ppm): 10.124 (s, 1H, –CHO), 9.05 (s, 1H, quinoline H-4), 7.58-8.53 (m, 8H, quinoline H-5, H-6, H-7, H-8 and phenyl protons); ^{13}C NMR (DMSO, 100 MHz, δ ppm): 192.985 (–CHO carbon atom), 123.420, 125.341, 126.373, 127.214, 127.119, 129.188, 130.120, 132.168, 133.161, 134.571, 135.463, 147.361, 147.398, 152.986, 159.929, 167.627, 168.221 (phenyl, quinoline and oxadiazole carbon atoms); HRMS, *m/z*: 378.2616 (M^+) (m.f.: $C_{18}H_{10}N_4O_4S$).

8-Methyl-2-((5-(4-nitrophenyl)-1,3,4-oxadiazol-2-yl)-thio)quinoline-3-carbaldehyde (7j): Yield: 74%, m.p.: 238-240 ºC; FT-IR (KBr, ν_{max}, cm^{-1}): 3068.75-2966.49 (aromatic C–H *str.*), 1696.9 (aldehyde C=O *str.*), 1588.34-1579.60 (oxadiazole and quinoline C=N *str.*), 1532.56 (phenyl C-NO_2 *str.*); 1497.57 (quinoline C–CH_3 *str.*); 1275.67 (oxadiazole C–O–C *str.*); ^{1}H NMR (DMSO, 400 MHz, δ ppm): 10.134 (s, 1H, –CHO), 8.93 (s, 1H, quinoline H-4), 7.58-8.53 (m, 7H, quinoline H-5, H-7, H-8 and phenyl protons), 2.532 (s, 3H, CH_3); ^{13}C NMR (DMSO, 100 MHz, δ ppm): 16.614 (–CH_3 carbon atom), 192.996 (–CHO carbon atom), 123.319, 125.484, 126.273, 127.114, 128.019, 129.088, 130.130, 132.058, 133.060, 134.461, 135.353, 147.352, 147.389, 152.995, 159.828, 167.526, 168.120 (phenyl, quinoline and oxadiazole carbon atoms); HRMS, *m/z*: 393.3612 (M^++1) (m.f.: $C_{19}H_{12}N_4O_4S$).

6-Chloro-2-((5-(4-nitrophenyl)-1,3,4-oxadiazol-2-yl)-thio)quinoline-3-carbaldehyde (7k): Yield: 66%, m.p.: 298-300 ºC; FT-IR (KBr, ν_{max}, cm^{-1}): 3069.75-2967.49 (aromatic C–H *str.*), 1698.23 (aldehyde C=O *str.*), 1590.54-1589.60 (oxadiazole and quinoline C=N *str.*), 1545.45 (phenyl C-NO_2 *str.*). 1276.57 (oxadiazole C–O–C *str.*), 736.58 (quinoline C–Cl *str.*); ^{1}H NMR (DMSO, 400 MHz, δ ppm): 10.145 (s, 1H, –CHO), 9.04 (s, 1H, quinoline H-4), 7.56-8.68 (m, 7H, quinoline H-5, H-6, H-7 and phenyl protons); ^{13}C NMR (DMSO, 100 MHz, δ ppm): 192.985 (–CHO carbon atom), 123.320, 125.330, 126.282, 127.125, 127.030, 129.092, 130.132, 132.169, 133.162, 134.561, 135.462, 147.362, 147.399, 152.987, 159.930, 167.626, 168.223 (phenyl, quinoline and oxadiazole carbon atoms); HRMS, *m/z*: 413.7970 (M^++1) (m.f.: $C_{18}H_9ClN_4O_4S$).

6-Methoxy-2-((5-(4-nitrophenyl)-1,3,4-oxadiazol-2-yl)-thio)quinoline-3-carbaldehyde (7l): Yield: 68%, m.p.: >300 ºC; FT-IR (KBr, ν_{max}, cm^{-1}): 3068.75-2971.49 (aromatic C–H *str.*), 1697.23 (aldehyde C=O *str.*), 1592.50-1591.64 (oxadiazole and quinoline C=N *str.*), 1548.55 (phenyl C-NO_2 *str.*), 1365.46 (quinoline C–OCH_3 *str.*), 1279.57 (oxadiazole C–O–C *str.*); ^{1}H NMR (DMSO, 400 MHz, δ ppm): 10.142 (s, 1H, –CHO), 8.96 (s, 1H, quinoline H-4), 7.70-8.53 (m, 7H, quinoline H-5, H-6, H-7 and phenyl protons), 3.98 (s, 1H, –OCH_3); ^{13}C NMR (DMSO, 100 MHz, δ ppm): 55.623 (–OCH_3 carbon atoms), 192.995 (–CHO carbon atom), 123.311, 125.330, 126.281, 127.132, 127.030, 129.097, 130.132, 132.169, 133.162, 134.562, 135.452, 147.362, 147.389, 152.986, 159.939, 167.635, 168.221 (phenyl, quinoline and oxadiazole carbon atoms); HRMS, *m/z*: 409.2879 (M^++1) (m.f.: $C_{19}H_{12}N_4O_5S$).

Antimicrobial activity studies

Antibacterial activity: The antibacterial activity of the newly synthesised oxadiazole linked quinolines (**7a-l**) were carried out against four different pathogenic organisms namely *Staphylococcus aureus*, *Bacillus subtilis* (Gram-positive) and *Escherichia coli* and *Pseudomonas aeruginosa* (Gram-negative). The antibacterial activity was assessed by determining the minimum inhibitory concentration (MIC) using the cup plate diffusion method [33]. Wells were aseptically created in the solidified nutrient agar medium using a sterile cork borer. An aliquot of 0.05 mL of test solution (1000 µg/mL) was dispensed into each well. Prior to well formation, the agar plates were uniformly inoculated with the test bacterial culture to ensure confluent growth. The plates were incubated at 37 ºC for 24 h, after which the zones of inhibition were measured in millimeters. Furacin was employed as the standard antibacterial agent and tested under identical experimental conditions at a concentration of 100 µg/mL. Nutrient agar served as the culture medium, while dimethylformamide (DMF) was used as the solvent control. The MIC was defined as the lowest concentration of the test compound at which no visible turbidity was observed, indicating complete inhibition of bacterial growth.

Antifungal activity: Fungicidal activity was determined following the same protocol used for antibacterial activity. The antifungal activity was assessed using *Candida albicans* as the test organism and fluconazole served as the reference standard.

Computational methods: Density functional theory (DFT) calculations were performed to investigate the electronic structure and reactivity of the compounds using Gaussian 09 with the GaussView 6.0.16 interface. Geometry optimizations were carried out in the gas phase without symmetry constraints employing the 6-311++G(d,p) basis set to assess the reliability of different exchange-correlation method. Frontier molecular orbital energies (HOMO and LUMO) and global reactivity descriptors were calculated according to Koopmans' theorem [34,35]. Mulliken population analysis was employed to determine atomic charge distribution and identify potential reactive sites.

RESULTS AND DISCUSSION

The synthetic strategy adopted in this study involved a multistep reactions. Initially, methyl-4-substituted benzoates

(**2**) were synthesized *via* acid-catalyzed esterification of the corresponding 4-substituted benzoic acids (**1**) using methanol in the presence of conc. H_2SO_4. Subsequent treatment of these esters with hydrazine hydrate afforded the corresponding 4-substituted benzohydrazides (**3**). Cyclization of benzohydrazides with CS_2 under basic conditions, using KOH, led to the formation of 5-(4-substituted phenyl)-1,3,4-oxadiazole-2-thiols (**4**), following the reported protocol [36] (**Scheme-I**). In a parallel synthetic route, 6-/8-substituted-2-chloroquinoline-3-carbaldehydes (**6**) were synthesized *via* Vilsmeier-Haack formylation of the corresponding substituted acetanilides (**5**), employing DMF and $POCl_3$, as reported by Meth-Cohn *et al.* [37] (**Scheme-II**). Finally, the target compounds, namely novel 2-((5-(4-substituted phenyl)-1,3,4-oxadiazol-2-yl)thio)-6/8-substituted quinoline-3-carbaldehydes (**7**), were synthesized through nucleophilic substitution of 6/8-substituted-2-chloroquinoline-3-carbaldehydes (**6**) with 5-(4-substituted phenyl)-1,3,4-oxadiazole-2-thiols (**4**) in an alcoholic medium using pyridine as a base (**Scheme-III**).

All the target compounds were successfully characterized using standard spectroscopic techniques. As a representative example, the FT-IR spectrum of compound **7b** showed the aldehyde carbonyl (C=O) stretching band at 1677.3 cm^{-1}. The quinoline and oxadiazole C=N stretching absorption band was observed at 1677.3 and 1569.2 cm^{-1}, respectively. The C–S stretching for oxadiazole-S linkage absorption band observed at 1166.7 cm^{-1} and C–S (for quinoline-S linkage) stretching absorption band observed at 1080.9 cm^{-1}. The aromatic C–H stretching absorption was observed in the region 3037.8-2762.0 cm^{-1}. The quinoline C–CH_3 absorption band observed at 1487.23 cm^{-1}. ^{1}H NMR spectrum of compound **7b** showed a singlet at 2.612 integrating for three protons of –CH_3 group. The aldehyde (–CHO) proton appeared as a singlet at δ 10.241 ppm integrating for one proton. The quinoline H-4 proton appeared as a singlet at δ 9.123 ppm integrating for one proton. The signals due to the quinoline H-5 and H-7 protons mingled together and appeared as multiplet in the region of δ 8.015-8.048 ppm integrating for two protons. The signals due to quinoline H-8 proton and phenyl protons appeared as multiplet in the region δ 7.563-7.704 ppm for six protons. ^{13}C NMR spectrum of compound **7b** showed signal at δ 16.614 ppm for –CH_3 carbon atom and signal at 192.994 for –CHO carbon atom. Signals at 123.319, 125.484, 126.273, 127.114, 128.019, 129.088, 130.130, 132.058, 133.060, 134.461, 135.353, 147.352, 147.389, 152.995, 159.828, 167.526, 168.120 for phenyl, quinoline and oxadiazole carbon atoms. Finally, the mass spectrum (HRMS) of compound **7b** showed the molecular ion peak at *m/z*, 348.5474 (M^++1) (m.f. $C_{19}H_{13}N_3O_2S$) in agreement with the proposed structure.

Antimicrobial activity studies: Among the evaluated compounds, the majority exhibited appreciable antibacterial activity that was comparable to the reference standard. Notably, compound **7k**, bearing a *p*-nitrophenyl substituent at the 2-position of the oxadiazole moiety and a chloro substituent at the 6-position of quinoline ring, demonstrated pronounced antibacterial activity against all the tested microorganisms. In addition, compound **7g**, featuring a *p*-nitrophenyl substituent at the 2-position of oxadiazole nucleus along with a chloro substituent at the 6-position of quinoline moiety, also displayed significant antibacterial efficacy when compared with the standard drug (Table-1).

Similarly, the majority of the synthesized compounds also exhibited appreciable antifungal activity (Table-1). Notably, compounds **7g** and **7k** demonstrated the highest antifungal efficacy against *C. albicans*. This enhanced activity may be attributed to the presence of electron-withdrawing nitro and chloro substituents, which are known to influence lipophilicity and facilitate stronger interactions with fungal cellular targets.

Density functional theory (DFT) studies: Understanding electronic distribution and active sites is critical for predicting biological interactions. Accordingly, compound **7k**, the most biologically active member of the series, was subjected to DFT analysis. Gaussian calculations were used to determine key quantum descriptors, with particular emphasis on HOMO and LUMO to assess electron-donating and electron-accepting tendencies. The computed quantum chemical parameters of compound **7k** at the B3LYP/3-21G level are summarized in Table-2. The geometrical optimised structure and the energy diagram of HOMO and LUMO orbitals are shown in Figs. 1 and 2, respectively.

TABLE-1
ANTIBACTERIAL AND ANTIFUNGAL ACTIVITY DATA OF COMPOUNDS **7a-l**

Compd. No.	R	R_1	Antibacterial activity (MIC, µg/mL)				Antifungal activity (MIC, µg/mL)
			E. coli	*S. aureus*	*P. aeruginosa*	*B. subtilis*	*C. albicans*
7a	H	H	17	18	18	20	19
7b	H	8-Methyl	20	18	17	19	19
7c	H	6-Chloro	22	22	23	21	23
7d	H	6-Methoxy	21	20	19	20	22
7e	Cl	H	22	20	22	21	22
7f	Cl	8-Methyl	23	23	22	22	23
7g	Cl	6-Chloro	25	26	25	24	26
7h	Cl	6-Methoxy	25	24	26	22	25
7i	NO_2	H	24	24	24	23	25
7j	NO_2	8-Methyl	23	24	25	23	23
7k	NO_2	6-Chloro	25	26	24	25	26
7l	NO_2	6-Methoxy	24	24	23	22	25
Furacin			24	23	24	22	–
Flucanazol			–	–	–	–	24

TABLE-2
DFT AT B3LYP/3-21G EMPLOYED FOR
7k QUANTUM CHEMICAL CALCULATIONS

Parameters	Expression	Value
Ionisation potential (I)	$I = -E_{HOMO}$	6.889280 eV
Electron affinity (A)	$A = -E_{LUMO}$	3.091441 eV
Energy gap (ΔE)	$\Delta E = E_{LUMO} - E_{HOMO}$	3.797839 eV
Electronegativity (χ)	$\chi = -(E_{HOMO} + E_{LUMO})/2$	4.990360 eV
Chemical potential (μ)	$\mu = -\chi$	-4.990360 eV
Global hardness (η)	$\eta = I - A/2$	1.898919 eV
Global softness (S)	$S = 1/\eta$	0.526680 eV
Electrophilicity index (ω)	$\omega = \mu^2/2\eta$	6.557334 eV

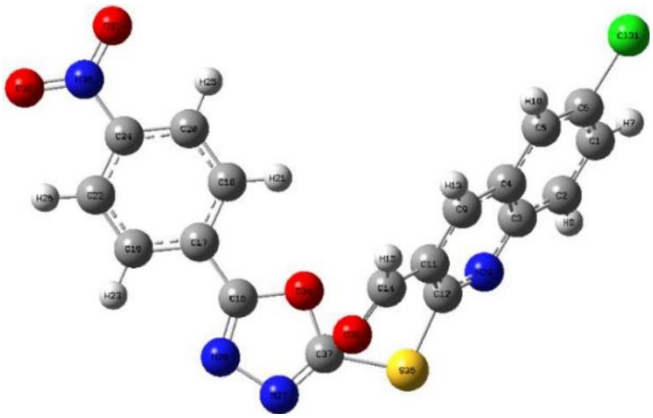

Fig. 1. Optimised structure of **7k**

Compound **7k** exhibited a relatively small HOMO–LUMO energy gap (3.7978 eV), indicating enhanced chemical reactivity and potential biological activity. The reduced chemical hardness (1.8989 eV) and high negative chemical potential (-4.9904 eV) suggest a soft and highly polarizable molecular system. The elevated electronegativity (4.9904 eV) and electrophilicity index (6.5573 eV) further indicate a strong tendency to accept electrons, supporting its role as an effective electrophile. The LUMO distribution was notably influenced by the chloro substituent on the quinoline ring, highlighting its contribution to electronic stabilization and reactivity.

The optimized structure of compound **7k** with Mulliken charge distribution is shown in Fig. 3, and the corresponding atomic charges are listed in Table-3. Mulliken population analysis revealed that all hydrogen atoms possess positive charge

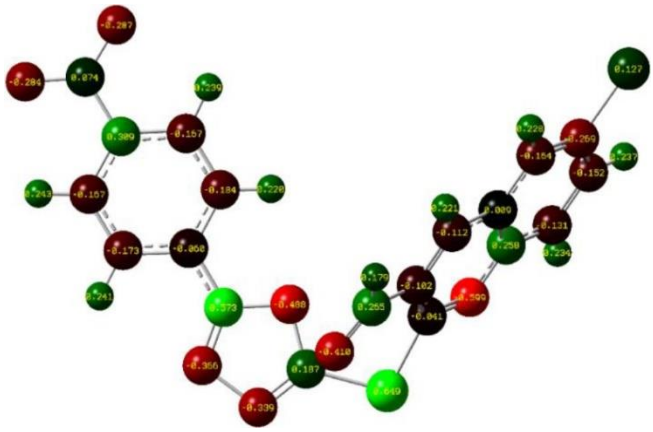

Fig. 3. Structure of **7k** with Mulliken charges

TABLE-3
ATOMS OF THE COMPOUND **7k** SHOWING MULLIKEN CHARGE (B3LYP/3-21G (d,p) RESULTS *in vacuo*)

Individual atom	Mulliken charge	Individual atom	Mulliken charge
1 C	-0.151904	20 C	-0.166729
2 C	-0.130623	21 H	0.220302
3 C	0.258224	22 C	-0.167084
4 C	0.009428	23 H	0.240779
5 C	-0.163861	24 C	0.309354
6 C	-0.269485	25 H	0.238948
7 H	0.237227	26 H	0.243269
8 H	0.233640	27 N	-0.338757
9 C	-0.112199	28 N	-0.365539
10 H	0.228095	29 N	-0.599338
11 C	-0.102176	30 N	0.074362
12 C	-0.040791	31 Cl	0.126704
13 H	0.220634	32 O	-0.286806
14 C	0.265187	33 O	-0.283836
15 H	0.179380	34 O	-0.487601
16 C	0.572566	35 O	-0.410274
17 C	-0.060218	36 S	0.648514
18 C	-0.184179	37 C	0.187394
19 C	-0.172605		

Sum of Mulliken charges = 0.00000

character. Among the carbon atoms, C6 exhibited the highest negative charge (-0.2695), while C16 showed the highest positive charge (0.5726). The nitrogen atoms displayed the most

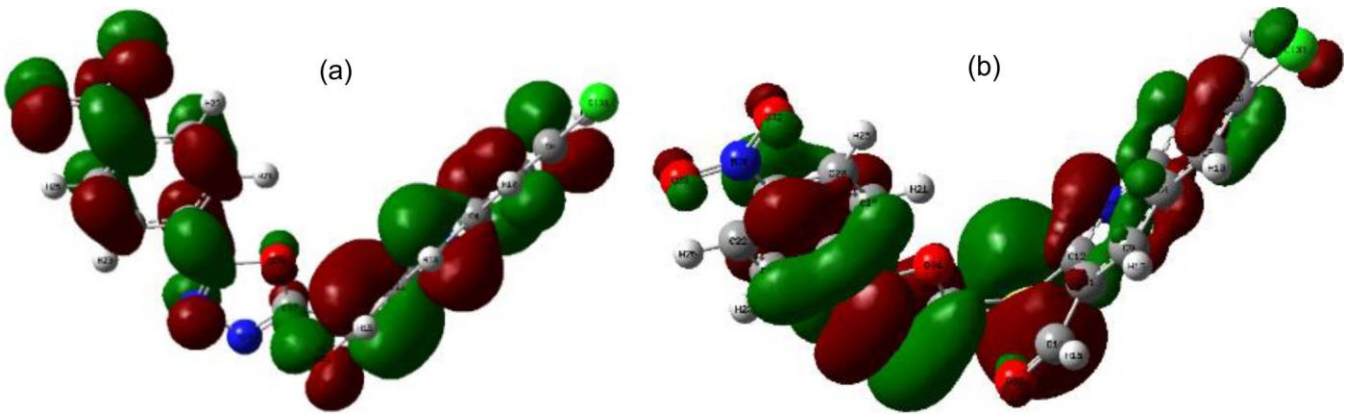

Fig. 2. Structure of **7k** showing distributions of (a) HOMO energy and (b) LUMO energy

pronounced negative charge density (up to -0.5993), indicating their potential involvement in intermolecular interactions and contributing to the enhanced antibacterial and antifungal activity of compound **7k**.

Conclusion

A new series of oxadiazole-linked quinoline-3-carbaldehyde derivatives (**7a-l**) was successfully synthesized through efficient multistep reactions and characterized. The antimicrobial evaluation revealed that most of the synthesized compounds exhibited promising antibacterial and antifungal activities, with several derivatives showing activity comparable to standard drugs. Among the series, compounds **7g** and **7k** emerged as the most potent antibacterial and antifungal agent, displaying broad-spectrum activity against both Gram-positive and Gram-negative bacteria as well as *Candida albicans*. The enhanced antimicrobial efficacy of these compounds can be attributed to the synergistic electronic effects of the nitro-substituted oxadiazole moiety and the chloro-substituted quinoline scaffold, highlighting the importance of strategic functional group modification. DFT studies provided the molecular-level insights into the observed biological activity. The lower HOMO–LUMO energy gap, reduced chemical hardness, and higher electrophilicity of compound **7k** indicate increased chemical reactivity and favourable electronic characteristics for biological interactions. Mulliken population analysis further identified heteroatoms and specific carbon centers as potential reactive sites, supporting the experimental antimicrobial findings.

ACKNOWLEDGEMENTS

The authors are thankful to Department of Chemistry, NMAM Institute of Technology, Nitte, for providing research facilities. The authors are also thankful to Central Instrumentation and Research Facility, Institution of Excellence, University of Mysore, Mysuru for providing NMR and Mass spectral analysis.

CONFLICT OF INTEREST

The authors declare that there is no conflict of interests regarding the publication of this article.

DECLARATION OF AI-ASSISTED TECHNOLOGIES

During the preparation of this manuscript, the authors used an AI-assisted tool(s) to improve the language. The authors reviewed and edited the content and take full responsibility for the published work.

REFERENCES

1. É. Frank and G. Szőllősi, *Molecules*, **26**, 4617 (2021); https://doi.org/10.3390/molecules26154617
2. F. Wang, Y. Yao, H.-L. Zhu and Y. Zhang, *Curr. Top. Med. Chem.*, **21**, 439 (2021); https://doi.org/10.2174/1568026621062103041056 31
3. P.V. Ledade, T.L. Lambat, J.K. Gunjate, P.K.P.G. Chopra, A.V. Bhute, M.R. Lanjewar, P.M. Kadu, U.J. Dongre and S.H. Mahmood, *Curr. Org. Chem.*, **27**, 206 (2023); https://doi.org/10.2174/1385272827666221227120648
4. Y.-Q. Zhao, X. Li, H.-Y. Guo, Q.-K. Shen, Z.-S. Quan and T. Luan, *Molecules*, **28**, 6478 (2023); https://doi.org/10.3390/molecules28186478
5. N.D. Chavan, S. Sarveswari and V. Vijayakumar, *RSC Adv.*, **15**, 30576 (2025); https://doi.org/10.1039/d5ra00534e
6. A. Lilienkampf, J. Mao, B. Wan, Y. Wang, S.G. Franzblau and A.P. Kozikowski, *J. Med. Chem.*, **52**, 2109 (2009); https://doi.org/10.1021/jm900003c
7. P. Nasveld and S. Kitchener, *Trans. R. Soc. Trop. Med. Hyg.*, **99**, 2 (2005); https://doi.org/10.1016/j.trstmh.2004.01.013
8. P.A. Leatham, H.A. Bird, V. Wright, D. Seymour and A. Gordon, *Eur. J. Rheumatol. Inflamm.*, **6**, 209 (1983).
9. W.A. Denny, W.R. Wilson, D.C. Ware, G.J. Atwell, J.B. Milbank and R.J. Stevenson, Anti-Cancer 2,3-Dihydro-1H-Pyrrolo[3,2-F]quinoline Complexes of Cobalt and Chromium, US Patent US007064117B2 (2006).
10. A. Mahamoud, J. Chevalier, A. Davin-Regli, J. Barbe and J.M. Pages, *Curr. Drug Targets*, **7**, 843 (2006); https://doi.org/10.2174/138945006777709557
11. N. Muruganantham, R. Sivakumar, N. Anbalagan, V. Gunasekaran and J.T. Leonard, *Biol. Pharm. Bull.*, **27**, 1683 (2004); https://doi.org/10.1248/bpb.27.1683
12. M.P. Maguire, K.R. Sheets, K. McVety, A.P. Spada and A. Zilberstein, *J. Med. Chem.*, **37**, 2129 (1994); https://doi.org/10.1021/jm00040a003
13. N. Ahmed, K.G. Brahmbhatt, S. Sabde, D. Mitra, I.P. Singh and K.K. Bhutani, *Bioorg. Med. Chem.*, **18**, 2872 (2010); https://doi.org/10.1016/j.bmc.2010.03.015
14. L. Strekowski, J.L. Mokrosz, V.A. Honkan, A. Czarny, M.T. Cegla, R.L. Wydra, S.E. Patterson and R.F. Schinazi, *J. Med. Chem.*, **34**, 1739 (1991); https://doi.org/10.1021/jm00109a031
15. K. Rana, Salahuddin and J.K. Sahu, *Curr. Drug Res. Rev.*, **13**, 90 (2021); https://doi.org/10.2174/2589977512666201221162627
16. M.A. Robichaud, A.I. Chiasson, J.A. Doiron, M.P.A. Hébert, M.E. Surette and M. Touaibia, *Drug Dev. Res.*, **86**, e70099 (2025); https://doi.org/10.1002/ddr.70099
17. P. Karegoudar, M.S. Karthikeyan, D.J. Prasad, M. Mahalinga, B.S. Holla and N.S. Kumari, *Eur. J. Med. Chem.*, **43**, 261 (2008); https://doi.org/10.1016/j.ejmech.2007.03.014
18. O. Prakash, M. Kumar, R. Kumar, C. Sharma and K.R. Aneja, *Eur. J. Med. Chem.*, **45**, 4252 (2010); https://doi.org/10.1016/j.ejmech.2010.06.023
19. A.A. El-Emam, O.A. Al-Deeb, M. Al-Omar and J. Lehmann, *Bioorg. Med. Chem.*, **12**, 5107 (2004); https://doi.org/10.1016/j.bmc.2004.07.033
20. S.G. Kucukguzel, E.E. Oruc, S. Rollas, F. Sahin and A. Ozbek, *Eur. J. Med. Chem.*, **37**, 197 (2002); https://doi.org/10.1016/S0223-5234(01)01326-5
21. P.R. Kagthara, N.S. Shah, R.K. Doshi and H.H. Parekh, *Indian J. Chem.*, **38B**, 572 (1999).
22. A. Mohd, S.A. Javed and H. Kumar, *Indian J. Chem.*, **46B**, 1014 (2007).
23. M. Akhter, A. Husain, B. Azad and M. Ajmal, *Eur. J. Med. Chem.*, **44**, 2372 (2009); https://doi.org/10.1016/j.ejmech.2008.09.005
24. A. Zarghi, S.A. Tabatabai, M. Faizi, A. Ahadian, P. Navabi, V. Zanganeh and A. Shafiee, *Bioorg. Med. Chem. Lett.*, **15**, 1863 (2005); https://doi.org/10.1016/j.bmcl.2005.02.014
25. D. Kumar, S. Sundaree, E.O. Johnson and K. Shah, *Bioorg. Med. Chem. Lett.*, **19**, 4492 (2009); https://doi.org/10.1016/j.bmcl.2009.03.172
26. S. Patil and S. Bhandari, *Mini Rev. Med. Chem.*, **22**, 805 (2022); https://doi.org/10.2174/1389557521666210902160644
27. S.M. Patil and S.V. Bhandari, *Anti-Cancer Agents Med. Chem.*, **20**, 779 (2023); https://doi.org/10.2174/1570180819666220414102310
28. N. Shruthi, B. Poojary, V. Kumar, M.M. Hussain, V.M. Rai, V.R. Pai, M. Bhat and B.C. Revannasiddappa, *RSC Adv.*, **6**, 8303 (2016); https://doi.org/10.1039/C5RA23282A

29. G. Bhasker, Salahuddin, A. Mazumder, R. Kumar, G. Kumar, M.J. Ahsan, M.S. Yar, F. Khan and B. Kapoor, *Curr. Org. Synth.*, **21**, 976 (2024); https://doi.org/10.2174/0115701794260740231010111408
30. V. Basavanna, M. Chandramouli, C. Kempaiah, U.K. Bhadraiah, N.S. Chandra, N.S. Lingegowda, S. Doddamani and S. Ningaiah, *Russ. J. Gen. Chem.*, **91**, 2257 (2021); https://doi.org/10.1134/S1070363221110128
31. V. Sharma, R. Das, D.K. Mehta and D. Sharma, *Mol. Divers.*, **29**, 1911 (2025); https://doi.org/10.1007/s11030-024-10949-y
32. J. Nayak, R.S. Bhat and D.M. Chethan, *ChemistrySelect*, **7**, e202103543c (2022); https://doi.org/10.1002/slct.202103543
33. H.W. Seely and P.J. Van Denmark, Microbes in Action: A Laboratory Manual in Microbiology, edn. 2, pp. 55-80 (1975).
34. S. Martinez, *Mater. Chem. Phys.*, **77**, 97 (2002); https://doi.org/10.1016/S0254-0584(01)00569-7
35. C.B.P. Kumar, M.K. Prashanth, K.N. Mohana, M.B. Jagadeesha, M.S. Raghu, N.K. Lokanath, Mahesha and K.Y. Kumar, *Surf. Interfaces*, **18**, 100446 (2020); https://doi.org/10.1016/j.surfin.2020.100446
36. A. Hasan, S. Gapil and I. Khan, *Asian J. Chem.*, **23**, 2007 (2011).
37. O. Meth-Cohn, B. Narine, B. Tarnowski, R. Hayes, A. Keyzad, S. Rhouati and A. Robinson, *J. Chem. Soc. Perkin Trans. I*, 1580 (1981); https://doi.org/10.1039/P19810002509